

**Study of exclusive processes  $e^+e^- \rightarrow VP$** V. V. Braguta,<sup>\*</sup> A. K. Likhoded,<sup>+</sup> and A. V. Luchinsky<sup>‡</sup>*Institute for High Energy Physics, Protvino, Russia*

(Received 25 August 2008; published 31 October 2008)

This paper is devoted to consideration of the hard exclusive processes  $e^+e^- \rightarrow VP$ , where  $V = \rho, \phi$ ;  $P = \eta, \eta'$ . Experimental measurement of the cross section of the process  $e^+e^- \rightarrow \phi\eta$  at the *BABAR* Collaboration at large center of mass energy  $\sqrt{s} = 10.6$  GeV and some low energy experimental data  $\sqrt{s} \sim 2-4$  GeV give us the possibility to study the cross section in the broad energy region. As a result, we have determined the asymptotic behavior of the cross section of  $e^+e^- \rightarrow \phi\eta$  in the limit  $s \rightarrow \infty$ , which is in agreement with perturbative QCD prediction. Assuming that the same asymptotic behavior is valid for the other processes under consideration and using low energy experimental data, we have predicted the cross sections of these processes at energies  $\sqrt{s} = 3.67, 10.6$  GeV. In addition, we have calculated the cross sections of these processes at the same energies within perturbative QCD. Our results are in agreement with available experimental data.

DOI: 10.1103/PhysRevD.78.074032

PACS numbers: 12.38.-t, 12.38.Bx, 13.66.Bc

**I. INTRODUCTION**

Exclusive hadron production in high energy electron-positron annihilation is a very interesting task for theoretical and experimental investigations. The presence of high energy scale  $\sqrt{s}$  that is much greater than the typical hadronic scale allows one to separate the amplitude of such processes into the hard part (creation of quarks at very small distances) and soft part (subsequent hadronization of these quarks into experimentally observed mesons at larger distances). The first part of the amplitude can be calculated within perturbative QCD. The second part of the amplitude is described by distribution amplitudes (DAs), which contain nonperturbative properties of final hadrons.

The description of hard exclusive hadron production within this pattern gives some very interesting predictions of the properties of hard exclusive processes [1,2]. One such prediction is the asymptotic behavior of the amplitudes and cross sections of hard exclusive processes in the limit  $s \rightarrow \infty$  [3–5]. It turns out that this behavior is determined by the perturbative part of amplitude and quantum numbers of final hadrons and does not depend on DAs of final hadrons.

To give the quantitative prediction for the cross section of the hard exclusive process, one needs to know DAs. It is interesting to note that if DAs are known, the theory can equivalently well predict the cross sections for the production of hadrons composed of light ( $u, d, s$  quarks) or heavy quarks ( $b, c$  quarks). There is a well known example of an exclusive process with heavy quarkonia production  $e^+e^- \rightarrow J/\Psi\eta_c$  measured by the Belle [6] and *BABAR* [7] collaborations. This process was extensively studied in many papers [8–17] with different approaches, which led

to a better understanding of charmonia properties and production processes. It is important to note that the approach to hard exclusive processes described above leads to a reasonable agreement with the experiments.

In this paper we study the processes  $e^+e^- \rightarrow VP$ , where  $V = \rho, \phi$ ;  $P = \eta, \eta'$ . Experimental measurement of the cross section of the process  $e^+e^- \rightarrow \phi\eta$  at the *BABAR* Collaboration at large center of mass energy  $\sqrt{s} = 10.6$  GeV and some low energy experimental data  $\sqrt{s} \sim 2-4$  GeV allow us to study the cross section of this process in the broad energy region. Our first purpose is to use these data in order to determine the asymptotic behavior of the cross section of the process  $e^+e^- \rightarrow \phi\eta$ . Assuming that the same asymptotic behavior is valid for the other processes under consideration and using low energy experimental data, one can predict the cross sections of the  $e^+e^- \rightarrow VP$  at energies  $\sqrt{s} = 3.67, 10.6$  GeV. In addition, we apply the perturbative QCD approach to estimate the values of the cross sections for the processes under consideration.

This paper is organized as follows. In the next section we analyze the experimental data for the process  $e^+e^- \rightarrow \phi\eta$  and determine the asymptotic behavior of this cross section. Then we apply the result of this study to predict the cross sections of the other processes under consideration at the center of mass energies  $\sqrt{s} = 3.67, 10.6$  GeV. In Sec. III we give theoretical predictions for the cross sections  $\sigma(e^+e^- \rightarrow \rho^0\eta)$ ,  $\sigma(e^+e^- \rightarrow \rho^0\eta')$ ,  $\sigma(e^+e^- \rightarrow \phi\eta)$ , and  $\sigma(e^+e^- \rightarrow \phi\eta')$  at  $\sqrt{s} = 3.67$  GeV and 10.6 GeV and compare them with available experimental data. The final section is devoted to the discussion of the results of this paper.

**II. THE ASYMPTOTIC BEHAVIOR**

The amplitude of the process involved can be written in the following form:

<sup>\*</sup>braguta@mail.ru<sup>+</sup>Likhoded@ihep.ru<sup>‡</sup>Alexey.Luchinsky@ihep.ru

$$\mathcal{M}(e^+e^- \rightarrow VP) = 4\pi\alpha \frac{\bar{v}(q_1)\gamma^\mu u(q_2)}{s} \langle V(p_1, \lambda)P(p_2) | J_\mu^{\text{em}} | 0 \rangle \times |J_\mu^{\text{em}} | 0 \rangle,$$

where  $\alpha$  is the electromagnetic coupling constant,  $u(q_2)$  and  $\bar{v}(q_1)$  are electron and positron bispinors,  $s = (q_1 + q_2)^2$  is the invariant mass of the  $e^+e^-$  system squared, and  $J_\mu^{\text{em}}$  is electromagnetic current. The matrix element  $\langle VP | J_\mu^{\text{em}} | 0 \rangle$  can be parametrized by the only form factor  $F(s)$ :

$$\langle V(p_1, \lambda)P(p_2) | J_\mu^{\text{em}} | 0 \rangle = ie_{\mu\nu\alpha\beta} \epsilon_\lambda^\nu p_1^\alpha p_2^\beta F(s), \quad (1)$$

where  $\epsilon_\lambda^\nu$  is the polarization vector of meson  $V$ . The cross section of the process under consideration equals

$$\sigma(e^+e^- \rightarrow VP) = \frac{\pi\alpha^2}{6} \left( \frac{2|\mathbf{p}|}{\sqrt{s}} \right)^3 |F(s)|^2. \quad (2)$$

In the last formula  $\mathbf{p}$  is the momentum of the vector meson  $V$  in the center of mass frame of final mesons.

In this section we will be interested in the asymptotic behavior of the form factor  $F(s)$  in the high energy region. Typical diagrams of the process under consideration are shown in Fig. 1. The asymptotic behavior of the diagram shown in Fig. 1(a) is  $\sigma \sim 1/s^2$ . At extremely large energies this diagram gives the dominant contribution. However, the amplitude of this diagram is suppressed by the smallness of the electromagnetic coupling constant, and our study shows that in the energy region analyzed in this paper the contribution of this diagram is negligible. Furthermore, let us consider the diagrams shown in Figs. 1(b) and 1(c). According to perturbative QCD [2] amplitudes (1) from such diagrams have the following asymptotic behavior:

$$\langle H_1(p_1, \lambda_1)H_2(p_2, \lambda_2) | J_\mu^{\text{em}} | 0 \rangle \sim \left( \frac{1}{\sqrt{s}} \right)^{|\lambda_1 + \lambda_2| + 1},$$

where  $H_1$  and  $H_2$  are mesons with momenta  $p_1$ ,  $p_2$  and helicities  $\lambda_1$  and  $\lambda_2$ . For the process under consideration  $H_1$  and  $H_2$  are the vector and pseudoscalar mesons, re-

spectively. The helicity of the pseudoscalar meson is, obviously,  $\lambda_2 = 0$ . Because of the antisymmetric tensor in (1), longitudinal polarization of the vector meson is forbidden, and it is transversely polarized ( $\lambda_1 = \pm 1$ ). So we have  $F(s) \sim 1/s^2$ ,  $\sigma(e^+e^- \rightarrow VP) \sim 1/s^4$ . On the other hand, in papers [18,19], it was stated that experimental data can be described only by the dependence  $\sigma \sim 1/s^3$ . To clarify this situation we will parametrize the form factor  $F(s)$  by the expression

$$F(s) = \frac{a_n(s)}{(\sqrt{s})^n}, \quad (3)$$

where  $a_n(s)$  slightly depends on  $s$  due to power and logarithmic corrections to the leading asymptotic behavior. Later in this section we will neglect such dependence. This approximation allows us to fix the constants  $a_n$  from the low energy data and predict the cross sections at  $\sqrt{s} = 3.67$  GeV and 10.6 GeV. We check three different hypotheses ( $n = 3, 4$ , and 5) and compare the results with existing experimental data.

First we are going to consider the process  $e^+e^- \rightarrow \phi\eta$ . To fix the constants  $a_n$  one can use low energy data [20]. When the constants  $a_n$  for different hypotheses are fixed, one can use them to predict the cross section in the high energy region and then compare this prediction with available high energy data [21] measured by the *BABAR* Collaboration:

$$\sigma_{\text{BABAR}}(e^+e^- \rightarrow \phi\eta) = 2.9 \pm 0.5 \text{ fb.}$$

Our results are shown in Fig. 2 and Table I. From this figure and table it can be clearly seen that only  $n = 4$  satisfactorily describes low and high energy experimental *BABAR* data [20,21]. This result is in agreement with the predictions of perturbative QCD. From Fig. 2 one can see that low energy CLEO-c data [22] are in disagreement with hypotheses  $n = 3, 4$ . Only hypothesis  $n = 5$  does not contradict the experimental results. However, if we assume that this hypothesis is correct, we will be faced with a dramatic contradiction with the high energy *BABAR* data

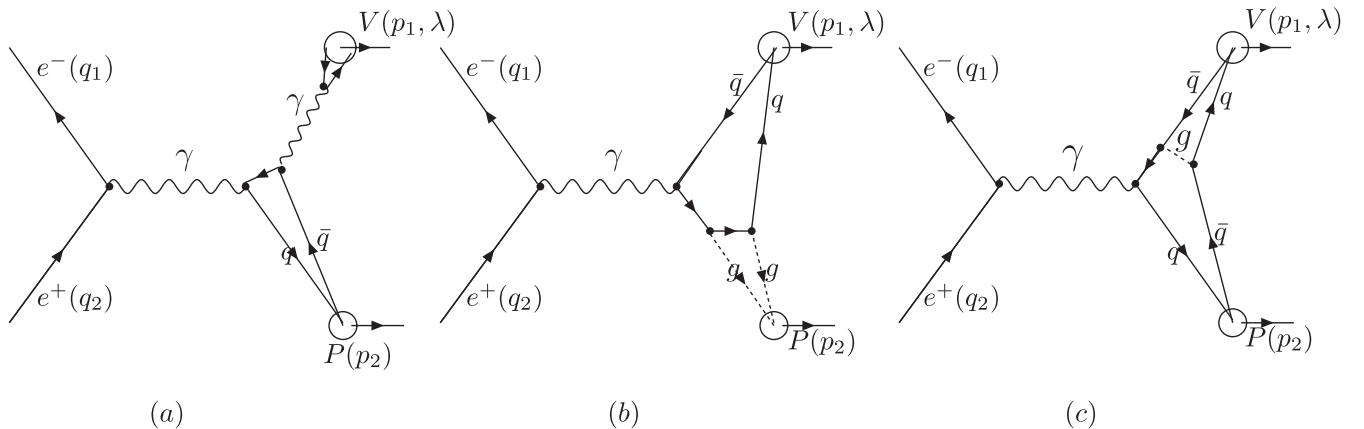


FIG. 1. Typical diagrams for the  $e^+e^- \rightarrow VP$  process.

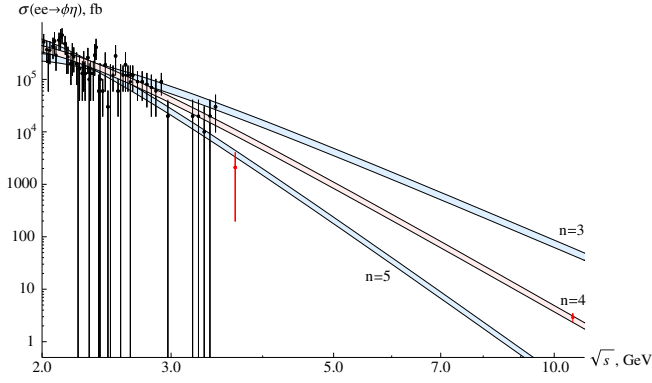


FIG. 2 (color online). Different hypotheses on the energy dependence for the  $\sigma(e^+e^- \rightarrow \phi\eta)$ . The constants  $a_n$  are fixed from the experimental values of this cross section in the low energy region ( $2 \text{ GeV} \leq \sqrt{s} \leq 3.5 \text{ GeV}$ ).

(see Fig. 2 and Table I). It should also be noted that in papers [18,19] it was stated that the energy dependence  $\sigma(e^+e^- \rightarrow \phi\eta) \sim 1/s^3$  describes experimental data more accurately. We believe that the disagreement of this statement with our conclusion arises from the fact that the authors of papers [18,19] did not take into account the low energy experimental result [20].

In view of this the question arises: is it possible to use the asymptotic behavior of the cross section (3) in the region  $\sqrt{s} \in (2, 3.5) \text{ GeV}$ . First, one can estimate the cross uncertainty due to the power corrections as  $\sim M^2/s$ . Even for the heaviest meson  $\phi$  and the smallest  $\sqrt{s}$  from the region  $\sqrt{s} \in (2, 3.5)$ , the error is  $\sim 0.25\%$ . We can also determine the size of power corrections from the fitting data [20] by the asymptotic form (3) plus the next-to-leading-order power correction. Our analysis shows that the uncertainty is not greater than  $10\% \sim 20\%$ . We believe that these

arguments confirm the applicability of the asymptotic expression for the cross section.

Now let us consider the processes  $e^+e^- \rightarrow \rho\eta, e^+e^- \rightarrow \rho\eta'$ . Unfortunately at the moment only the low energy CLEO-c data [22] are available for these processes. As seen from Table I the experimental error of these data is rather large. More precise experimental data can be obtained from the decays  $J/\psi \rightarrow \rho\eta, J/\psi \rightarrow \rho\eta'$ . The corresponding branching fractions are equal to [23]

$$\text{Br}(e^+e^- \rightarrow \rho\eta) = (1.93 \pm 0.23) \times 10^{-4},$$

$$\text{Br}(e^+e^- \rightarrow \rho\eta') = (1.05 \pm 0.18) \times 10^{-4}.$$

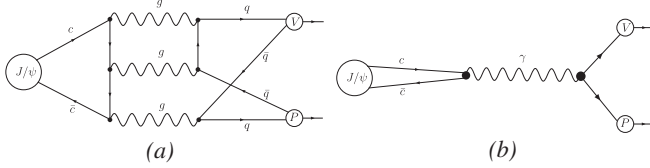
Generally speaking, these decays can proceed both via strong and electromagnetic interaction (see Fig. 3 for the typical diagrams). Because of the isospin violation, however, the gluon induced diagrams are strongly suppressed, and the purely electromagnetic diagram gives the dominant contribution. The branching fractions of these decays are equal to

$$\begin{aligned} \text{Br}(J/\psi \rightarrow VP) &= \left( \frac{|p|}{M_{J/\psi}} \right)^3 \left| \frac{a_n(M_{J/\psi}^2)}{M_{J/\psi}^n} \right|^2 M_{J/\psi}^2 \\ &\times \text{Br}(J/\psi \rightarrow e^+e^-). \end{aligned} \quad (4)$$

From this relation we can determine the value of the function  $a_n(M_{J/\psi}^2)$  and, neglecting energy dependence in  $a_n(s)$  (this assumption leads to additional errors, which can be estimated as  $\sim M^2/s \sim 10\%$ ), predict the cross sections of the processes  $e^+e^- \rightarrow \rho\eta$  and  $e^+e^- \rightarrow \rho\eta'$  over the large energy region. The results are shown in Figs. 4 and 5 and Table I. From these results it is seen that the low energy data do not allow an understanding of what hypotheses agree best with the experiments. So to determine the asymptotic behavior unambiguously the high energy data

TABLE I. The constants  $a_n$  and the cross sections at  $\sqrt{s} = 3.67$  and  $10.6 \text{ GeV}$  in comparison with the experimental data. The second column contains the constants  $a_{3,4,5}$  for the different final states, obtained from the low energy data. In the third and fifth columns the experimental results for the cross sections  $\sigma(e^+e^- \rightarrow VP)$  at the center of mass energy  $\sqrt{s} = 3.67 \text{ GeV}$  and  $\sqrt{s} = 10.6 \text{ GeV}$  are presented. The results of the calculation are shown in the fourth and sixth columns.

$VP$	Parameters	$\sigma(\sqrt{s} = 3.67 \text{ GeV}) \text{ pb}$		$\sigma(\sqrt{s} = 10.6 \text{ GeV}) \text{ fb}$	
		Exp.	Fit results	Exp.	Fit results
$\rho\eta$	$a_3 = 1.8 \pm 0.2 \text{ GeV}^2$	$10 \pm 2.5$	$12 \pm 3$	...	$24 \pm 6$
	$a_4 = 5.6 \pm 0.7 \text{ GeV}^3$		$8 \pm 2$		$2.1 \pm 0.5$
	$a_5 = 17.3 \pm 2.1 \text{ GeV}^4$		$6 \pm 1$		$0.18 \pm 0.04$
$\rho\eta'$	$a_3 = 1.5 \pm 0.2 \text{ GeV}^2$	$2.1 \pm 1.6$	$7 \pm 2$	...	$17 \pm 4$
	$a_4 = 4.7 \pm 0.6 \text{ GeV}^3$		$5 \pm 3$		$1.4 \pm 0.4$
	$a_5 = 14.5 \pm 1.9 \text{ GeV}^4$		$3.5 \pm 0.9$		$0.12 \pm 0.03$
$\phi\eta$	$a_3 = 2.7 \pm 0.2 \text{ GeV}^2$	$2.1 \pm 1.9$	$23 \pm 4$	$2.9 \pm 0.5$	$52 \pm 8$
	$a_4 = 6.4 \pm 0.4 \text{ GeV}^3$		$9.8 \pm 1.3$		$2.7 \pm 0.4$
	$a_5 = 14.8 \pm 1.1 \text{ GeV}^4$		$3.8 \pm 0.5$		$0.13 \pm 0.02$
$\phi\eta'$	$a_3 = 0.76 \pm 0.06 \text{ GeV}^2$	$<12.6$	$1.5 \pm 0.2$	...	$4.2 \pm 0.7$
	$a_4 = 8.1 \pm 0.7 \text{ GeV}^3$		$12.8 \pm 2.1$		$4.2 \pm 0.7$
	$a_5 = 85 \pm 7 \text{ GeV}^4$		$110 \pm 18$		$4.2 \pm 0.7$

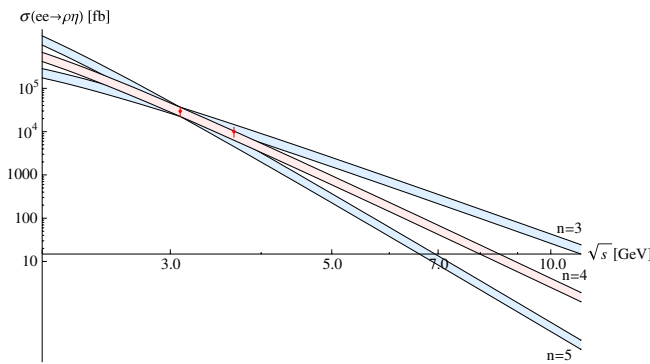
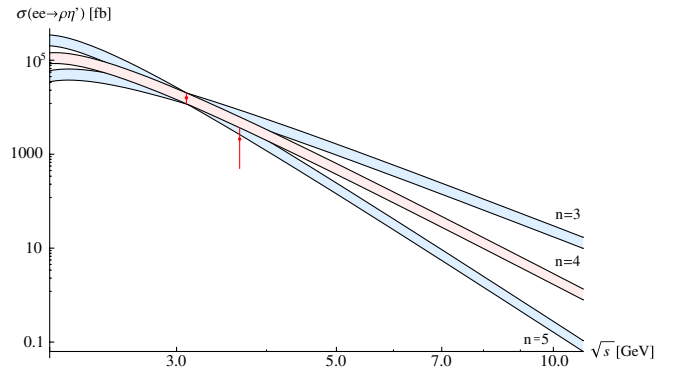

FIG. 3. Typical diagrams for  $J/\psi \rightarrow VP$  decay.

are needed. However, if we assume that the asymptotic behavior for the cross section of the process  $e^+e^- \rightarrow \phi\eta$  is the same as that for the processes  $e^+e^- \rightarrow \rho\eta$ ,  $e^+e^- \rightarrow \rho\eta'$ , we can predict the cross sections of these processes at energies  $\sqrt{s} = 3.67, 10.6$  GeV:

$$\begin{aligned} \sigma_{\sqrt{s}=3.67 \text{ GeV}}(e^+e^- \rightarrow \rho\eta) &= 8 \pm 2 \text{ pb}, \\ \sigma_{\sqrt{s}=3.67 \text{ GeV}}(e^+e^- \rightarrow \rho\eta') &= 5 \pm 3 \text{ pb}, \\ \sigma_{\sqrt{s}=10.6 \text{ GeV}}(e^+e^- \rightarrow \rho\eta) &= 2.1 \pm 0.5 \text{ fb}, \\ \sigma_{\sqrt{s}=10.6 \text{ GeV}}(e^+e^- \rightarrow \rho\eta') &= 1.4 \pm 0.4 \text{ fb}. \end{aligned} \quad (5)$$

The cross sections at the energy  $\sqrt{s} = 3.67$  GeV are in agreement with the CLEO-c data.

Let us now proceed with the reaction  $e^+e^- \rightarrow \phi\eta'$ . In this case experimental information is even more poor. One cannot use the branching fraction of the decay  $\text{Br}(J/\psi \rightarrow \phi\eta')$ , since in this case isospin is conserved and the diagram shown in Fig. 3(a) gives the main contribution to  $J/\psi \rightarrow \phi\eta'$  decay. In addition, CLEO-c gives us only the upper bound on the cross section  $\sigma(e^+e^- \rightarrow \phi\eta')$ , and no experimental information in the high energy region is available. Using  $\eta$ - $\eta'$  mixing it is possible, however, to estimate the cross section  $\sigma(e^+e^- \rightarrow \phi\eta')$  from the value of the  $e^+e^- \rightarrow \phi\eta$  cross section. The mixing of pseudoscalar mesons can be described by different parametrizations [24]. In our paper we will use the parametrization of  $\eta$ - $\eta'$  mixing in the quark flavor basis with one mixing angle [25]:


FIG. 4 (color online). Different hypotheses on the energy dependence for the  $\sigma(e^+e^- \rightarrow \rho\eta)$ . The constants  $a_n$  are fixed from the  $J/\psi \rightarrow \rho\eta$  branching fraction [the rightmost point represents the cross section at  $\sqrt{s} = M_{J/\psi}$  calculated using relations (2)–(4)].

FIG. 5 (color online). Different hypotheses on the energy dependence for the  $\sigma(e^+e^- \rightarrow \rho\eta')$ . The constants  $a_n$  are fixed from the  $J/\psi \rightarrow \rho\eta'$  branching fraction [the rightmost point represents the cross section at  $\sqrt{s} = M_{J/\psi}$  calculated using relations (2)–(4)].

$$\begin{pmatrix} \eta \\ \eta' \end{pmatrix} = \begin{pmatrix} \cos\Phi & -\sin\Phi \\ \sin\Phi & \cos\Phi \end{pmatrix} \begin{pmatrix} \eta_n \\ \eta_s \end{pmatrix}, \quad (6)$$

where  $\eta_n = (u\bar{u} + d\bar{d})/\sqrt{2}$  and  $\eta_s = s\bar{s}$  represent the basis of the quark mixing scheme. Using this mixing scheme it is easy to obtain the following relation between  $e^+e^- \rightarrow \phi\eta$  and  $e^+e^- \rightarrow \phi\eta'$  cross sections:

$$\frac{\sigma(e^+e^- \rightarrow \phi\eta')}{\sigma(e^+e^- \rightarrow \phi\eta)} = \cot^2\Phi.$$

There are plenty of theoretical and experimental works dedicated to the determination of the mixing angle. The well known estimation, based on Gell-Mann-Okubo mass formulas, gives the value of  $\Phi$  at about  $32^\circ$  for the linear mass formula and about  $45^\circ$  for a quadratic case. The analysis of the axial anomaly generated decays  $\eta, \eta' \rightarrow \gamma\gamma$  was performed in papers [26,27] and the estimate  $\Phi = 30^\circ \div 35^\circ$  was obtained. In papers [28,29] another anomaly based investigation of a large set of decay processes was performed and the value  $\Phi = 38^\circ \pm 2^\circ$  was presented. The authors of the recent work [30] used the dispersive approach to  $\eta$ - $\eta'$  mixing and obtained the value

$$\Phi = 39.4^\circ \pm 1^\circ.$$

It is interesting to note that this value is close to phenomenological value  $\Phi = 39.3^\circ \pm 1^\circ$ , presented in the pioneering work [25]. We will use this value of the mixing angle in our article. The error of this angle is small in comparison with the error in the  $e^+e^- \rightarrow \phi\eta$  cross section.

Knowing the value of the cross section  $\sigma(e^+e^- \rightarrow \phi\eta)$  one can determine the value of the cross section  $\sigma(e^+e^- \rightarrow \phi\eta')$  at the energy  $\sqrt{s} = 10.6$  GeV.

$$\sigma_{\sqrt{s}=10.6 \text{ GeV}}(e^+e^- \rightarrow \phi\eta') = 4.2 \pm 0.7 \text{ fb}.$$

From this we can calculate the value of the constants  $a_n$  for different hypotheses and predict the cross section of the process  $e^+e^- \rightarrow \phi\eta'$  in the low energy region. We show

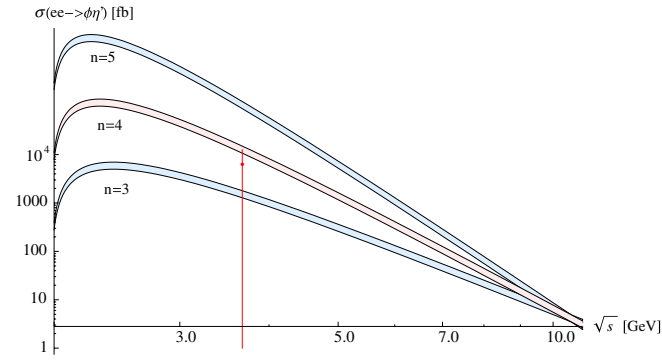


FIG. 6 (color online). Different hypotheses on the energy dependence for the  $\sigma(e^+e^- \rightarrow \phi\eta')$ . The constants  $a_n$  are fixed from the experimental values of this cross section at  $\sqrt{s} = 10.6$  GeV.

the energy dependence of this cross section in Fig. 6. From this figure one sees that the value  $n = 5$  contradicts experimental results at  $\sqrt{s} = 3.67$  GeV, while  $n = 3$  and  $n = 4$  do not. From theoretical arguments and the analysis presented above of the  $e^+e^- \rightarrow \phi\eta$  reaction, we think that the value  $n = 4$  is more preferable. For this hypothesis we can predict the value of the cross section at energy  $\sqrt{s} =$

3.67 GeV,

$$\sigma_{\sqrt{s}=3.67 \text{ GeV}}(e^+e^- \rightarrow \phi\eta') = 12.8 \pm 2.1 \text{ pb},$$

which does not contradict the CLEO-c data.

In Table I we present the results of this section. The second column contains the constants  $a_{3,4,5}$  for different final states, obtained from low energy fits. In the third and fifth columns experimental results for the cross sections  $\sigma(e^+e^- \rightarrow VP)$  at the center of mass energies  $\sqrt{s} = 3.67$  GeV and 10.6 GeV are presented. The results of the calculation are shown in the fourth and sixth columns. From this table it is clear that only relation  $\sigma \sim 1/s^4$  agrees with experiments.

### III. CALCULATION OF THE CROSS SECTIONS

#### A. Numerical parameters and distribution amplitudes

Now let us try to estimate the cross sections of the processes studied in the last section theoretically. To calculate the cross sections of the processes  $e^+e^- \rightarrow VP$  for  $V = \phi, \rho, P = \eta, \eta'$ , one needs to know the DAs of final mesons. For the vector mesons the DAs needed in the calculation can be written as [2,13]

$$\begin{aligned} \langle V_\lambda(p) | \bar{q}_\beta(z) q_\alpha(-z) | 0 \rangle_\mu &= \frac{f_V M_V}{4} \int_0^1 dx e^{i(pz)(2x-1)} \left\{ \hat{p} \frac{(e_\lambda z)}{(pz)} V_L(x) + \left( \hat{e}_\lambda - \hat{p} \frac{(e_\lambda z)}{(pz)} \right) V_\perp(x) + \frac{f_T(\mu)}{f_V M_V} (\sigma_{\mu\nu} e_\lambda^\mu p^\nu) V_T(x) \right. \\ &\quad \left. + \frac{1}{2} (\epsilon_{\mu\nu\alpha\beta} \gamma_\mu \gamma_5 e_\lambda^\nu p^\alpha z^\beta) V_A(x) \right\}_{\alpha\beta}, \end{aligned} \quad (7)$$

where  $x$  is the fraction of momentum carried by the quark and  $f_V, f_T(\mu), M_V$  are the leptonic, tensor constants and the mass of vector meson. In the calculation the  $\phi$  meson is assumed to be composed of  $s$  quarks, so in (7)  $q = s$ . For the  $\rho^0$  meson isospin 1 combination  $\bar{q}q = (\bar{u}u - \bar{d}d)/\sqrt{2}$  is assumed. The models for DAs and the decay constants  $f_V, f_T(\mu)$  for  $\phi$  and  $\rho$  mesons will be taken from paper [31].

In the framework of the quark mixing scheme (6) the decay constants

$$\begin{aligned} \langle P(p) | \bar{n} \gamma^\mu \gamma_5 n | 0 \rangle &= i f_P^n p^\mu, \\ \langle P(p) | \bar{s} \gamma^\mu \gamma_5 s | 0 \rangle &= i f_P^s p^\mu, \end{aligned}$$

needed in the calculation can be expressed through the constants

$$\begin{aligned} \langle P(p) | \bar{n}_\beta(z) n_\alpha(-z) | 0 \rangle_\mu &= i \frac{f_P^n M_P}{4} \int_0^1 dy e^{i(pz)(2y-1)} \left\{ \frac{\hat{p} \gamma_5}{M_P} P_A^n(y) - f_P^n(\mu) \gamma_5 P_P^n(y) \right\}, \\ \langle P(p) | \bar{s}_\beta(z) s_\alpha(-z) | 0 \rangle_\mu &= i \frac{f_P^s M_P}{4} \int_0^1 dy e^{i(pz)(2y-1)} \left\{ \frac{\hat{p} \gamma_5}{M_P} P_A^s(y) - f_P^s(\mu) \gamma_5 P_P^s(y) \right\}, \end{aligned}$$

where

$$\langle \eta_n(p) | \bar{n} \gamma^\mu \gamma_5 n | 0 \rangle = i f^n p^\mu,$$

$$\langle \eta_s(p) | \bar{s} \gamma^\mu \gamma_5 s | 0 \rangle = i f^s p^\mu,$$

as follows:

$$\begin{pmatrix} f_\eta^n & f_\eta^s \\ f_{\eta'}^n & f_{\eta'}^s \end{pmatrix} = \begin{pmatrix} \cos\Phi & -\sin\Phi \\ \sin\Phi & \cos\Phi \end{pmatrix} \begin{pmatrix} f^n & 0 \\ 0 & f^s \end{pmatrix}.$$

In turn, the constants  $f^n, f^s$  and the mixing angle  $\Phi$  can be determined from experiment [25]:

$$f^n = (1.07 \pm 0.02) f_\pi, \quad f^s = (1.34 \pm 0.06) f_\pi.$$

Within this mixing pattern the DAs needed in the calculation can be written in the following form [2,13]:

$$f_p^n(\mu) = \frac{1}{2m_n(\mu)} \left[ m_\eta^2 \cos^2 \Phi + m_{\eta'}^2 \sin^2 \Phi - \frac{\sqrt{2}f^s}{f^n} (m_{\eta'}^2 - m_\eta^2) \cos \Phi \sin \Phi \right],$$

$$f_p^s(\mu) = \frac{1}{2m_s(\mu)} \left[ m_\eta^2 \cos^2 \Phi + m_{\eta'}^2 \sin^2 \Phi - \frac{f^n}{\sqrt{2}f^s} (m_{\eta'}^2 - m_\eta^2) \cos \Phi \sin \Phi \right].$$

The calculation will be done with the masses  $m_s(1 \text{ GeV}) = 150 \text{ MeV}$ ,  $m_n(1 \text{ GeV}) = (m_u(1 \text{ GeV}) + m_d(1 \text{ GeV}))/2 = 5 \text{ MeV}$ , and it will be assumed that  $P_A^s(y) = P_A^n(y) = P_A(y)$  and  $P_P^s(y) = P_P^n(y) = P_P(y)$ . The models of the leading twist DAs  $P_A$  for the  $\eta$  and  $\eta'$  mesons will be taken from paper [32]. For the function  $P_P(y)$  the asymptotic form will be used.

It should be noted that the wave functions and the constants introduced above depend on the renormalization scale  $\mu$ . Our calculation shows that the scale dependence of the DAs is not very important, and below it will be ignored. At the same time the scale dependence of the constants is important, and it will be taken into account. The calculation will be done at the scale  $\mu = \sqrt{s}/2$ .

## B. Numerical results and discussion

Having introduced the designations of the DAs one can proceed with the calculation of the cross sections. First we are going to consider the diagrams similar to that shown in Fig. 1(a). It is not difficult to calculate the contribution of these diagrams to the form factor  $F(s)$ :

$$|F(s)| = \frac{4\pi\alpha}{s} \frac{f_V}{M_V} \left( \frac{e_u^2 + e_d^2}{\sqrt{2}} f_P^n + e_s^2 f_P^s \right) \int_0^1 \frac{dy}{y_1 y_2} P_A(y),$$

where  $e_u, e_d, e_s$  are the charges of  $u, d, s$  quarks correspondingly. For the process  $e^+e^- \rightarrow \phi\eta$  at the energy  $\sqrt{s} = 10.6 \text{ GeV}$  we have  $\sigma = 0.01 \text{ fb}$ , which is by 2 orders of magnitude less than the experimental result. From this it is clear that the contribution of the diagram shown in Fig. 1(a) is negligible, and below it will be ignored. It should be noted that in the limit  $s \rightarrow \infty$  the contribution of the Fig. 1(a) diagram to the cross section has the following behavior:  $\sim 1/s^2$ . So at extremely large energy this diagram gives the dominant contribution. Our calculation shows that this happens at energies  $\sqrt{s} \geq 35 \text{ GeV}$ .

Now we are going to consider the other diagrams shown in Fig. 1. The leading asymptotic behavior of these diagrams is  $\sigma \sim 1/s^4$ . First, it should be noted that the contribution of the diagram shown in Fig. 1(b) is very small [18], and it will be ignored below. This fact results from the rather small admixture of the  $|GG\rangle$  Fock state in the pseudoscalar mesons  $\eta, \eta'$ . Now we proceed to the calculation of the diagram shown in Fig. 1(c). The contribution of this diagram to the  $F(s)$  for the processes under study can be written as follows [13]:

$$|F_{\phi\eta}(s)| = \frac{32\pi}{9} \frac{f_V f^s M_V \sin \Phi}{s^2} e_s I_0,$$

$$|F_{\phi\eta'}(s)| = \frac{32\pi}{9} \frac{f_V f^s M_V \cos \Phi}{s^2} e_s I_0,$$

$$|F_{\rho\eta}(s)| = \frac{32\pi}{9} \frac{f_V f^n M_V \cos \Phi}{2s^2} (e_u - e_d) I_0,$$

$$|F_{\rho\eta'}(s)| = \frac{32\pi}{9} \frac{f_V f^n M_V \sin \Phi}{2s^2} (e_u - e_d) I_0.$$

In the above expressions

$$I_0 = \int_0^1 dx \int_0^1 dy \alpha_s(\mu) \left\{ \frac{f_t(\mu)}{M_V} f_p(\mu) \frac{V_T(x) P_P(y)}{x^2 y} \right. \\ \left. + \frac{1}{2} \frac{V_L(x) P_A(y)}{xy} + (1-2y) \frac{V_\perp(x) P_A(y)}{xy^2} \right. \\ \left. + \frac{1}{8} \frac{(1+y) V_A(x) P_A(y)}{x^2 y^2} \right\},$$

where  $f_t(\mu) = f_T(\mu)/f_V$ ,  $f_p(\mu) = f_p^s(\mu)$  for the processes with  $\phi$  meson in the final state and  $f_p(\mu) = f_p^n(\mu)$  for the processes with  $\rho$  meson in the final state.

The following point deserves consideration. The models for the DAs that we use in our calculation are truncated series in Gegebauer polynomials. This means that the end point behavior ( $x \rightarrow 0, 1$ ) of these DAs coincides with the end point behavior of the corresponding asymptotic DAs. From this it is not difficult to see that the integral  $I_0$  is logarithmically divergent. One way to regularize this divergence is to introduce cutoff parameter  $x_0$ . In our calculation we take the following value of cutoff parameter  $x_0 = \Lambda/\sqrt{s}$ .  $\Lambda$  is of order of the typical hadronic scale, which is of order of several hundred MeV. The physical meaning of this cutoff can be understood as follows: if  $x \sim x_0$  quark momentum is of order of  $\sim \Lambda$ , and in this region one must take into account transverse motion in hadron that regularizes the whole integral  $I_0$ . The parameter  $\Lambda$  can be determined from available experimental results. We determined this parameter from the cross section of the process  $e^+e^- \rightarrow \phi\eta$  at  $\sqrt{s} = 10.6 \text{ GeV}$ . Thus we get  $\Lambda = 130_{-17}^{+25} \text{ MeV}$ . The variation of the parameter  $\Lambda$  corresponds with  $1\sigma$  deviation from the central value measured by the Belle Collaboration.

The results of the calculation are shown in Table II. The second and fifth columns contain the experimental results for the cross sections at the energies  $\sqrt{s} = 3.67 \text{ GeV}$  and  $\sqrt{s} = 10.6 \text{ GeV}$  correspondingly. The results obtained in paper [18] are shown in the third and sixth columns. The results obtained in this paper are shown in the fourth and

TABLE II. The results of the calculation. The second and fifth columns contain experimental results for the cross sections at energies  $\sqrt{s} = 3.67$  GeV and  $\sqrt{s} = 10.6$  GeV correspondingly. The results obtained in paper [18] are shown in the third and sixth columns. The results obtained in this paper are shown in the fourth and seventh columns.

$VP$	$\sigma(\sqrt{s} = 3.67 \text{ GeV}) \text{ pb}$			$\sigma(\sqrt{s} = 10.6 \text{ GeV}) \text{ fb}$		
	Exp. [22]	[18]	This work	Exp. [21]	[18]	This work
$\rho\eta$	$10 \pm 2.5$	$8.1 \div 16.6$	$3.7 \div 6.3$	...	$2.4 \div 3.1$	$2.4 \div 3.5$
$\rho\eta'$	$2.1 \pm 1.6$	$4.3 \div 8.6$	$2.1 \div 3.6$	...	$1.5 \div 2.1$	$1.6 \div 2.3$
$\phi\eta$	$2.1 \pm 1.9$	$9.6 \div 19.1$	$3.7 \div 6.1$	$2.9 \pm 0.5$	$3.3 \div 4.3$	$2.4 \div 3.4$
$\phi\eta'$	$<12.6$	$11.5 \div 22.6$	$4.6 \div 7.6$	...	$4.4 \div 5.8$	$3.5 \div 5.0$

seventh columns. The variations of the results are due to the variation in parameter  $\Lambda$ . It is seen from this table that the results of the calculation are in satisfactory agreement with the experiment.

It should be noted here that in addition to the diagrams shown in Fig. 1, there is an additional contribution to the form factor  $F(s)$  which was not considered in this paper. This contribution appears if one takes into account the higher Fock state of the vector and pseudoscalar mesons  $|q\bar{q}G\rangle$  and its asymptotic behavior is also  $\sigma \sim 1/s^4$ . This contribution was considered in papers [2,33]. In paper [2] the authors asserted that the Fock state  $|q\bar{q}G\rangle$  gives a very important contribution to the cross section and must be taken into account. Contrary to this conclusion, the author of paper [33] asserted that the main contribution arises from the diagram shown in Fig. 1(c). So the question about the role of higher Fock state  $|q\bar{q}G\rangle$  in the total cross section deserves separate consideration, and it will not be considered here.

#### IV. DISCUSSION AND CONCLUSION

In this work we have studied the production of light mesons  $\rho\eta$ ,  $\rho\eta'$ ,  $\phi\eta$ , and  $\phi\eta'$  in the high energy electron-positron annihilation.

The first question studied in this paper is the asymptotic behavior of the cross sections of the processes under consideration. Perturbative QCD predicts that the cross section of the reaction  $e^+e^- \rightarrow VP$  has the asymptotic behavior  $\sigma \sim 1/s^4$  in the limit  $s \rightarrow \infty$ . Experimental measurement of the cross section of the process  $e^+e^- \rightarrow \phi\eta$  at the large center of mass energy  $\sqrt{s} = 10.6$  GeV [21] and

the low energy experimental data  $\sqrt{s} \sim 2-4$  GeV [20] give us the possibility to study the cross section in the broad energy region. As a result, we have determined the asymptotic behavior of the cross section of  $e^+e^- \rightarrow \phi\eta$  in the limit  $s \rightarrow \infty$ , which is in agreement with perturbative QCD prediction. As to the other processes under study, there are no high energy experimental data which allow us to confirm perturbative QCD prediction for these processes. We would like to stress here that the high energy experimental data turned out to be crucial in the determination of the asymptotic behavior of the cross sections. Assuming that the asymptotic behavior predicted by perturbative QCD is valid for the other processes under consideration, we have calculated the cross sections of the processes  $e^+e^- \rightarrow \rho\eta$ ,  $\rho\eta'$ ,  $\phi\eta$ ,  $\phi\eta'$  at the energies  $\sqrt{s} = 3.67, 10.6$  GeV.

In addition, we have applied the perturbative QCD approach to calculate the cross sections of the processes under study at the energies  $\sqrt{s} = 3.67$  GeV and  $\sqrt{s} = 10.6$  GeV. The results of this calculation are in satisfactory agreement with available experimental data.

#### ACKNOWLEDGMENTS

The authors would like to thank A. A. Sokolov and M. M. Shapkin for useful and stimulating discussions. This work was partially supported by the Russian Foundation of Basic Research under Grant No. 07-02-00417. The work of V. Braguta was partially supported by CRDF Grant No. Y3-P-11-05 and President Grant No. MK-2996.2007.2. The work of A. Luchinsky was partially supported by President Grant No. MK-110.2008.2 and the Russian Science Support Foundation.

- [1] G. P. Lepage and S. J. Brodsky, Phys. Rev. D **22**, 2157 (1980).  
 [2] V. L. Chernyak and A. R. Zhitnitsky, Phys. Rep. **112**, 173 (1984).  
 [3] V. L. Chernyak, A. R. Zhitnitsky, and V. G. Serbo, Pis'ma Zh. Eksp. Teor. Fiz. **26**, 760 (1977) [JETP Lett. **26**, 594 (1977)].  
 [4] V. L. Chernyak and A. R. Zhitnitsky, Yad. Fiz. **31**, 1053

- (1980) [Sov. J. Nucl. Phys. **31**, 544 (1980)].  
 [5] V. L. Chernyak and A. R. Zhitnitsky, Pis'ma Zh. Eksp. Teor. Fiz. **25**, 544 (1977) [JETP Lett. **25**, 510 (1977)].  
 [6] K. Abe *et al.* (Belle Collaboration), Phys. Rev. Lett. **89**, 142001 (2002).  
 [7] B. Aubert *et al.* (BABAR Collaboration), Phys. Rev. D **72**, 031101 (2005).

- [8] K. Y. Liu, Z. G. He, and K. T. Chao, Phys. Lett. B **557**, 45 (2003).
- [9] K. Y. Liu, Z. G. He, and K. T. Chao, Phys. Rev. D **77**, 014002 (2008).
- [10] Y. J. Zhang, Y. j. Gao, and K. T. Chao, Phys. Rev. Lett. **96**, 092001 (2006).
- [11] Z. G. He, Y. Fan, and K. T. Chao, Phys. Rev. D **75**, 074011 (2007).
- [12] H. M. Choi and C. R. Ji, Phys. Rev. D **76**, 094010 (2007).
- [13] A. E. Bondar and V. L. Chernyak, Phys. Lett. B **612**, 215 (2005).
- [14] V. V. Braguta, A. K. Likhoded, and A. V. Luchinsky, Phys. Rev. D **72**, 074019 (2005).
- [15] E. Braaten and J. Lee, Phys. Rev. D **67**, 054007 (2003); **72**, 099901(E) (2005).
- [16] G. T. Bodwin, J. Lee, and C. Yu, Phys. Rev. D **77**, 094018 (2008).
- [17] J. P. Ma and Z. G. Si, Phys. Rev. D **70**, 074007 (2004).
- [18] C. D. Lu, W. Wang, and Y. M. Wang, Phys. Rev. D **75**, 094020 (2007).
- [19] J. M. Gerard and G. Lopez Castro, Phys. Lett. B **425**, 365 (1998).
- [20] B. Aubert *et al.* (BABAR Collaboration), Phys. Rev. D **76**, 092005 (2007); **77**, 119902(E) (2008).
- [21] B. Aubert *et al.* (BABAR Collaboration), Phys. Rev. D **74**, 111103 (2006).
- [22] N. E. Adam *et al.* (CLEO Collaboration), Phys. Rev. Lett. **94**, 012005 (2005).
- [23] W. M. Yao *et al.* (Particle Data Group), J. Phys. G **33**, 1 (2006).
- [24] T. Feldmann, Int. J. Mod. Phys. A **15**, 159 (2000).
- [25] T. Feldmann, P. Kroll, and B. Stech, Phys. Rev. D **58**, 114006 (1998); Phys. Lett. B **449**, 339 (1999).
- [26] J. F. Donoghue, B. R. Holstein, and Y. C. R. Lin, Phys. Rev. Lett. **55**, 2766 (1985); **61**, 1527(E) (1988).
- [27] F. J. Gilman and R. Kauffman, Phys. Rev. D **36**, 2761 (1987); **37**, 3348(E) (1988).
- [28] R. Akhoury and J. M. Frere, Phys. Lett. B **220**, 258 (1989).
- [29] P. Ball, J. M. Frere, and M. Tytgat, Phys. Lett. B **365**, 367 (1996).
- [30] Y. N. Klopot, A. G. Oganessian, and O. V. Teryaev, arXiv:0810.1217.
- [31] P. Ball, V. M. Braun, Y. Koike, and K. Tanaka, Nucl. Phys. **B529**, 323 (1998).
- [32] P. Kroll and K. Passek-Kumericki, Phys. Rev. D **67**, 054017 (2003).
- [33] A. S. Gorsky, Moscow Inst. Theor. Exp. Phys. GKAE, Report No. ITEF-85-071.